Toxicology Reports 9 (2022) 126–135

Contents lists available at ScienceDirect

Toxicology Reports

journal homepage: www.elsevier.com/locate/toxrep

Development of a thermal spray coating aerosol generator and inhalation exposure system

Aliakbar A. Afshari [a], Walter McKinney [a], Jared L. Cumpston [a], Howard D. Leonard [a], James B. Cumpston [a], Terence G. Meighan [a], Mark Jackson [a], Sherri Friend [a], Vamsi Kodali [a], Eun Gyung Lee [b], James M. Antonini [a,*]

[a] Health Effects Laboratory Division, National Institute for Occupational Safety and Health, Morgantown, WV, 26508, United States
[b] Respiratory Health Division, National Institute for Occupational Safety and Health, Morgantown, WV, 26508, United States

ARTICLE INFO

Handling Editor: Dr. Aristidis Tsatsakis

Keywords:
Thermal spray coating
Metals
Particulates
Particle size
Inhalation system

ABSTRACT

Thermal spray coating involves spraying a product (oftentimes metal) that is melted by extremely high temperatures and then applied under pressure onto a surface. Large amounts of a complex metal aerosol (e.g., Fe, Cr, Ni, Zn) are formed during the process, presenting a potentially serious risk to the operator. Information about the health effects associated with exposure to these aerosols is lacking. Even less is known about the chemical and physical properties of these aerosols. The goal was to develop and test an automated thermal spray coating aerosol generator and inhalation exposure system that would simulate workplace exposures. An electric arc wire-thermal spray coating aerosol generator and exposure system was designed and separated into two areas: (1) an enclosed room where the spray coating occurs; (2) an exposure chamber with different measurement devices and controllers. The physicochemical properties of aerosols generated during electric arc wire-thermal spray coating using five different consumable wires were examined. The metal composition of each was determined by inductively coupled plasma-atomic emission spectroscopy (ICP-AES), including two stainless-steel wires [PMET720 (82 % Fe, 13 % Cr); PMET731(66 % Fe, 26 % Cr)], two Ni-based wires [PMET876 (55 % Ni, 17 % Cr); PMET885 (97 % Ni)], and one Zn-based wire [PMET540 (99 % Zn)]. The particles generated regardless of composition were poorly soluble, complex metal oxides and mostly arranged as chain-like agglomerates and similar in size distribution as determined by micro-orifice uniform deposit impactor (MOUDI) and electrical low-pressure impactor (ELPI). To allow for continuous, sequential spray coating during a 4-hr exposure period, a motor rotated the metal pipe to be coated in a circular and up-and-down direction. In a pilot animal study, male Sprague-Dawley rats were exposed to aerosols (25 mg/m^3 × 4 h/d × 9 d) generated from electric arc wire-thermal spray coating using the stainless-steel PMET720 consumable wire. The targeted exposure chamber concentration was achieved and maintained during a 4-hr period. At 1 d after exposure, lung injury and inflammation were significantly elevated in the group exposed to the thermal spray coating aerosol compared to the air control group. The system was designed and constructed for future animal exposure studies to generate continuous metal spray coating aerosols at a targeted concentration for extended periods of time without interruption.

1. Introduction

Thermal spray coating is a surface treatment process that enables different types of materials to be deposited on various substrates, such as metal, metal alloys, ceramics, and plastics [1]. The process involves spraying a metal coating product, in wire or powder form, that is melted by extremely high temperatures (e.g., 2,600-16,000 °C) and then sprayed under pressure onto a surface [2]. Thermal spray processes are easy to use, cost little to operate, and have coating attributes that are beneficial to applications for numerous industries, such as automotive, gas and energy, medical, aerospace, steel, electronics, salvage and restoration, and consumer goods [1]. Applications include coatings for

* Corresponding author at: Centers for Disease Control & Prevention, National Institute for Occupational Safety and Health, Health Effects Laboratory Division, 1000 Frederick Lane (Mailstop 2015), Morgantown, WV, 26508, United States.
E-mail address: JGA6@cdc.gov (J.M. Antonini).

https://doi.org/10.1016/j.toxrep.2022.01.004
Received 23 November 2021; Received in revised form 10 January 2022; Accepted 21 January 2022
Available online 25 January 2022

wear prevention and sealing, restoration and decoration, thermal insulation, oxidation and corrosion resistance, and the fabrication of spray-formed parts, free-standing components, and nano-structured materials.

In most thermal spray coating processes, large amounts of metal aerosols composed of mostly fine and ultrafine particulates are formed [3,4], presenting a potentially serious risk to the operator who still in most cases performs the processes manually. The generated particles in thermal spray coating are most often composed of complex mixtures of pneumotoxic metals, such as chromium (Cr), nickel (Ni), zinc (Zn), and aluminum (Al). Unfortunately, information about the possible health effects associated with exposure to aerosols generated during thermal spray coating is unavailable or lacking. Even less is known about the chemical (e.g., metal composition, surface chemistry, solubility) and physical (e.g., particle size and morphology) properties of aerosols generated during thermal spray coating processes.

Workplace exposure to aerosols generated during thermal spray coating operations is an emerging hazard. The global market for thermal spray applications is projected to increase to 17 billion dollars by 2027 [1,5]. Nearly 138,000 workers were employed as coating and spraying machine operators in 2020 [6]. However, this number is expected to grow substantially as the demand for thermal spray coating increases. Airborne concentrations of toxic metals in workplaces during thermal spray coating have been observed to be substantially elevated. It has been reported that hexavalent Cr exposures "were as high as we have ever measured (>500 μg/m^3) in an open-air work area that approached 100 times the OSHA permissible exposure limit of 5 μg/m^3," (A. Siert, Xcel Energy, February, 2017; personal correspondence), "measured to be 20–40 times higher than the permissible exposure limit for a 12-hr work shift" (L.P. Dutton, Work Environment Associates, June, 2008; personal correspondence), and were 15 times higher than the French occupational exposure limit for sprayed materials containing Cr or Cr oxides in French worksites [7].

The goal of the project was to construct an automated, computer-controlled thermal spray coating aerosol generator and animal inhalation exposure system that would simulate actual workplace exposures and provide continuous metal spray coating for extended periods of time without interruption. Such a system would allow for reproducibility of the exposure, study of time- and dose-response relationships, and comparison of the toxicity of different types of thermal spray coating aerosols. This manuscript describes the development of a novel robotic thermal spray coating aerosol generator and inhalation exposure system and the physical and chemical characterization of the generated particles from different types of consumable wires.

2. Materials and methods

2.1. Thermal spray coating aerosol generation and exposure system

An automated, computer-controlled thermal spray coating particle generator and inhalation system was designed and constructed to perform animal studies to mimic workplace exposures. The design of the system was developed after the primary inhalation engineer (Dr. A. Afshari) on the project visited two facilities that performed thermal spray regularly and based on the recommendations suggested by experienced thermal spray operators. The electric arc wire- thermal spray coating aerosol generation and exposure system is separated into two areas (as depicted in the diagram in Fig. 1 and the images in Fig. 2): (A) an enclosed room where the spray coating occurs that contains a compressed air tank, thermal spray machine with wire holder and feeder unit (AT-400 Wire Arc Spray System; Thermach, Inc., Medina, WI), the rotary and reciprocating system that holds and rotates the stainless-steel pipe up and down to be spray-coated, and a spray coating booth that houses the torch gun and rotary sample holder system; (B) the exposure chamber with different measurement devices and controllers. The room that contains the thermal spray coating booth is isolated from the investigators by a set of protective curtains and glass door dividers to prevent exposure to the generated fumes and gases should the booth leak outward. The thermal spray coating was performed in the spray booth with the booth door closed.

The aerosols generated during the thermal spray coating process were delivered to an exposure chamber. The generated particles were pulled from the spay booth into an air-tight exposure chamber from a slight negative pressure, no more than 1.0" of H_2O differential. After leaving the booth, the fume passed through a large particle trap then mixed with an automatically adjusted amount of diluted air. After the

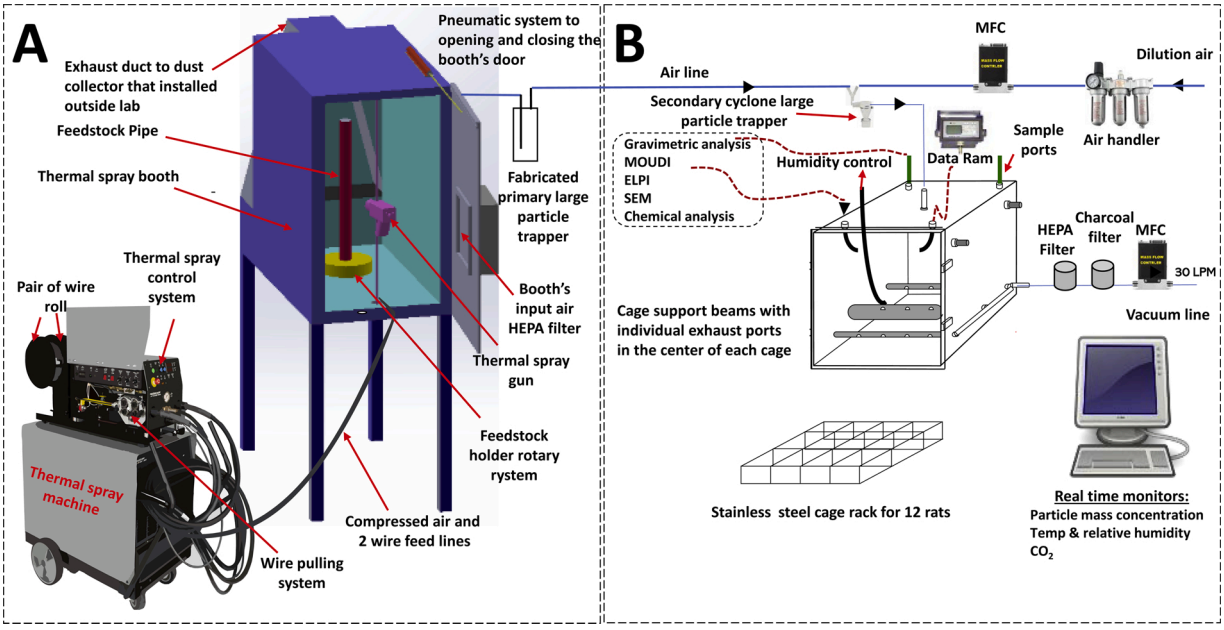

Fig. 1. Schematic diagram of the electric arc wire-thermal spray coating aerosol generator and exposure system (as modified from [4]). Electric arc wire- thermal spray coating was performed in one room (A), and the aerosols transferred to an animal exposure chamber in a separate room (B) divided by shaded glass doors (B). Abbreviations: Data Ram = real-time aerosol monitor; MOUDI = Micro Orifice Uniform Deposit Impactor; ELPI = electric low-pressure impactor; SEM = scanning electron microscopy; TEM = transmission electron microscopy; Temp = temperature; MFC = mass flow controller.

Fig. 2. Images of the completed thermal spray coating generator and exposure system, including the (A) compressed air tank and electric arc wire thermal spray machine with wire feeder; (B) closed spray booth; (C) opened spray booth with spray gun and metal pipe to be coated; (D) glass doors with protective curtains that separates the two rooms of the system; (E) animal exposure chamber with assorted air lines and sampling devices.

fume and dilution air mixed, it passed through a homemade particle remover and mixed by diluted air and passed through a cyclone (URG-2000-30EP, URG Corp, Chapel Hill NC) to further remove large particles. The cut size of this cyclone is 6 μm at a flow of 31 L/min. The flow into this cyclone was maintained at 31 L/min, by using a mass flow controller connected to the house vacuum on the exhaust side of the air-tight exposure chamber. Large particles were removed so that the animals would receive only the portion of the particles that was <6 μm. Throughout the manuscript when the term 'respirable particles' is mentioned, it refers to the portion of particles <6μm. Because of the possible role nanoparticles play in the resulting toxicological responses of the lungs after inhalation, the portion of particles <100 nm were not removed or controlled.

The mass concentration in the chamber was monitored by a real-time aerosol monitor (DataRAM, MIE, Inc. Bedford, MA). The sensors and measurement devices were managed and controlled through a custom computer software programed written in LabVIEW (National Instruments Corporation, Austin, TX). To maintain a constant particle concentration in the exposure chamber, the software would make adjustments to the amount of dilution air that made up the 31 L/min entering the exposure chamber. For example, if the concentration needed to be higher than its current level it would automatically lower the dilution air thus pulling more aerosol from the spray booth. The feedback control algorithm used to control the dilution air was a Proportional-Integral-Derivative feedback (PID) controller. The parameters of the PID controller were found by the trial-and-error tuning method. When the amount of dilution air dropped below 4 L/min the custom software would trigger first the feedstock pipe to rotate and move up and down in front of the thermal spray gun for few seconds before activating the thermal spray gun for a 1-sec spray. This would make the dilution air increase to keep the exposure concentration from climbing too high, then the amount of dilution air needed would slowly drop until it was below 4 L/min and another spray would trigger. This process would repeat, typically 1 spray every 5–20 min, until the end of the desired exposure duration. Particle mass concentrations inside the animal chamber were determined by collecting airborne particles with two 47-mm closed cassettes loaded with polytetrafluoroethylene filters followed by gravimetric analyses. This filter data was used every exposure run to validate and calibrate the DataRAM. The target exposure chamber mass concentration could be selected in the software and was typically set to 25–30 mg/m^3 for all experiments.

Additional ports were located on the top of the chamber and used to measure chamber pressure and to collect additional particle samples for size distribution, chemical composition, and for electron microscopy analysis. The air pressure and temperature and relative humidity inside the chamber were continually measured during the exposure period (Vaisala Temperature-Humidity Probe, model# HMP60; Woburn, MA). Also, the levels of generated carbon dioxide (Vaisala CO_2 Probe, model# GMP252; Woburn, MA) were monitored in the chamber during animal exposures.

The physicochemical properties of aerosols generated during electric arc wire-thermal spray coating using five different and commonly used consumable wires were examined (Table 1), including two stainless-

Table 1
Manufacturer specifications of consumable wires tested in the study.

Consumable wire type	Metal composition of wire - according to manufacturer (weight %)
PMET720	84.7 Fe, 13.0 Cr, 1.0 Mn
PMET731	69.8 Fe, 23.5 Cr, 5.3 Al, 0.45 Mn
PMET885	93.0 Ni, 5.3 Al
PMET876	60.0 Ni, 15.0 Cr, 16.0 Mo, 5.0 Fe, 4.0 W
PMET540	99.9 Zn

[1]Relative to all metals analyzed.

steel wires (PMET720 and PMET731; Polymet Corporation, West Chester, OH), two Ni-based wires (PMET876 and PMET885; Polymet Corporation), and one Zn-based wire (PMET540; Polymet Corporation). The spray coating process parameters used for each are included in Table 2. In addition, a study of PMET720 using two different compressed air pressures (50 and 60 psi) was performed to assess whether it affected the physical and/or chemical characteristics of the generated particles.

2.2. Thermal spray coating aerosol characterization

2.2.1. Particle size and morphology

The size distribution of the different thermal spray coating aerosols inside the exposure chamber were determined by two methods. The first method assessed particle size distribution by mass and used a Micro-Orifice Uniform Deposit Impactor (MOUDI; MSP Model 110, MSP Corporation, Shoreview, MN). Particles were collected between the size ranges of 0.056–18 μm that were separated into 11 stages where each stage was loaded with a 47-mm aluminum foil filter except for the filter stage. The mass median aerodynamic diameter (MMAD) and geometric standard deviation (GSD) of the aerosols were determined from gravimetric measurements. The second method assessed particle size distribution by number and used an electrical low-pressure impactor (Dekati ELPI; Particle Instruments, Vadnais Heights, MN) that measured airborne particle size distribution in real time in the size range of 6 nm - 10 μm at 10 Hz sampling rate. The count median aerodynamic diameter (CMAD) and particle surface area were determined by ELPI.

To assess particle morphology, the aerosolized particles from thermal spray coating were collected using 47-mm cassettes loaded with polycarbonate filters (0.2 μm pore size; Whatman, Clinton, PA). The filters loaded with particles were mounted onto aluminum stubs using double-stick carbon tape and viewed using a Hitachi S4800 field emission scanning electron microscope (SEM; Hitachi High-Tech America, Boston, MA). Elemental profiles of collected thermal spray coating particles were determined by energy dispersive X-ray spectroscopy analysis (EDX; Bruker Madison, WI) at 20 kV to map specific metal components of the particle samples.

2.2.2. Metal composition

Particle samples were collected inside the exposure chamber onto 5 μm pore size polyvinyl chloride membrane filters (SKC, inc., Eighty Four, PA) in 37-mm cassettes during thermal spray coating using the different consumable wires. The collected samples were analyzed for metal components by the NIOSH contract laboratory using inductively coupled plasma-atomic emission spectroscopy (ICP-AES) according to NIOSH Method 7303 modified for hot block/HCl/HNO_3 digestion [8]. Metal content of blank filters also were analyzed for control purposes.

2.3. Animals and exposure pilot study

Male Sprague-Dawley rats (250–300 g; Hilltop Lab Animals, Scottdale, PA) were used and free of viral pathogens, parasites, mycoplasmas, Helicobacter, and CAR bacillus. The rats were acclimated for one week after arrival and provided HEPA-filtered air, irradiated Teklad 2918 diet, and tap water *ad libitum*. All animal procedures used were reviewed and approved by the Centers for Disease Control and Prevention (CDC), Morgantown-National Institute for Occupational Safety and Health (NIOSH) Animal Care and Use Committee (ACUC). The animal facilities are specific pathogen-free, environmentally controlled, and accredited by the AAALAC International (Frederick, MD).

In a pilot study to test the system, the rats were exposed to the respirable portion of aerosols (25 mg/m^3 × 4 h/d × 9 d) generated from electric arc wire- thermal spray coating using a stainless-steel consumable wire (PMET720; Polymet Corporation, West Chester, OH) at settings of 200 A, 60 psi, and 30 V. PMET720 was chosen for study because

Table 2
Thermal spray coating parameters and measured aerosol characteristics.

Consumable Wire Type	Spray Coating Parameters	Metal Composition of Formed Aerosol (weight %)[1]	MOUDI MMAD (nm)	Geometric Std. Deviation	ELPI CMAD (nm)	Particle Surface Area ($\mu m^2/cm^3$)
PMET720 (stainless steel)	60 psi, 30 V, 200 A	Fe 82.2 ± 0.24 Cr 13.4 ± 0.14 Mn 2.37 ± 0.09 Zn 1.31 ± 0.13 Ni 0.397 ± 0.14 Cu 0.175 ± 0.013	306	2.11	103	1.54×10^6
PMET720 (stainless steel)	50 psi, 30 V, 200 A	Fe 81.7 ± 0.24 Cr 14.9 ± 0.19 Mn 2.61 ± 0.04 Zn 0.354 ± 0.08 Ni 0.260 ± 0.04 Cu 0.160 ± 0.002	280	1.83	96	8.70×10^5
PMET731 (stainless steel)	60 psi, 30 V, 200 A	Fe 66.3 ± 0.56 Cr 26.2 ± 0.57 Al 5.32 ± 0.15 Mn 1.02 ± 0.02 Zn 0.237 ± 0.05 Ni 0.289 ± 0.03 Cu 0.139 ± 0.03	310	1.94	104	1.03×10^6
PMET885 (Ni-based)	60 psi, 30 V, 250 A	Ni 96.9 ± 0.63 Al 1.69 ± 0.03 Zn 1.06 ± 0.32 Fe 0.699 ± 0.11 Ni 55.5 ± 0.46	316	1.94	111	1.12×10^6
PMET876 (Ni-based)	60 psi, 30 V, 200 A	Cr 17.4 ± 0.26 Mo 17.0 ± 0.58 Fe 5.08 ± 0.15 Mn 3.40 ± 0.07 Al 0.911 ± 0.04 Zn 0.649 ± 0.14	367	2.13	135	3.70×10^5
PMET540 (Zn- based)	60 psi, 23 V, 200 A	Zn 99.4 ± 0.24 Ni 0.325 ± 0.16 Fe 0.235 ± 0.14	378	1.89	165	9.15×10^5

[1] Relative to all metals analyzed; values are means ± standard error (n = 4).

it is the most common material used for repair and restoration in all thermal spray coating companies. Control animals were exposed to filtered air. The justification for the target particle concentration used in the study was that it fell in the range measured in workplaces where thermal spray coating occurred [7,9,23,24]. Also, it is a comparable concentration used in similar animal inhalation studies exposed to other metal particles such as welding fumes [10–12]. The aerosols were generated in a closed spray booth and transported to the exposure chamber. At 1 d after the final exposure, bronchoalveolar lavage (BAL) was performed to assess lung injury and inflammation. Animals were euthanized with an overdose of a pentobarbital-based euthanasia solution (>100 mg/kg body weight, IP; Fatal-Plus Solution, Vortech Pharmaceutical, Inc., Dearborn, MI, USA) and then exsanguinated by severing the abdominal aorta.

The right lung was first lavaged with a 1 ml/100 g body weight aliquot of calcium- and magnesium-free phosphate-buffered saline (PBS), pH 7.4. The first fraction of recovered bronchoalveolar lavage fluid (BALF) was centrifuged at 500×*g* for 10 min, and the resultant cell-free supernatant was saved for lung cell damage analysis. The right lung was further lavaged with 6-ml aliquots of PBS until 30 ml were collected. These samples also were centrifuged for 10 min at 500×*g* and the cell-free BALF discarded. The cell pellets from all washes for each rat were combined, washed, re-suspended in 1 ml of PBS buffer, counted, and differentiated.

For the determination of lung inflammation, total cell numbers recovered by BAL were determined using a Coulter Multisizer II and AccuComp software (Coulter Electronics, Hialeah, FL, USA). Cell suspensions (5×10^4 cells) were spun using a Cytospin 3 centrifuge (Shandon Life Sciences International, Cheshire, England) for 5 min at 800 rpm onto a slide. Cells (200/rat) were identified after labeling with Leukostat stain (Fisher Scientific, Pittsburgh, PA, USA) as monocytes/alveolar macrophages (AMs) and neutrophils (PMNs). In addition, lactate dehydrogenase (LDH) was measured in the first fraction of the cell-free supernatant recovered from the BALF as a general marker for lung cell injury. LDH activity was determined by measuring the oxidation of lactate to pyruvate coupled with the formation of NADH at 340 nm. Measurements were taken with a COBAS MIRA auto-analyzer (Roche Diagnostic Systems, Montclair, NJ, USA). Also, a rat cytokine 27-plex discovery assay (Eve Technologies Corp., Calgary, Canada) was performed on the recovered BALF to further assay the inflammatory response in the lungs.

2.4. Statistics

Lung response results were expressed as means ± standard error (n = 5–6). Statistical analysis was performed using SigmaStat (Systat Software, Inc., SigmaPlot for Windows, San Jose, CA). Comparisons between treatment groups was performed using a student *t*-test. Criterion for significance was set at $p < 0.05$.

3. Results

3.1. Thermal spray coating generator and exposure system

During double wire arc-spray coating, two consumable metal wires are fed independently into the spray gun within the spray booth (Fig. 3). A charge is formed between the wires, and an arc is generated between them. The extreme heat from the arc melts the incoming wires resulting in vaporized metal particle agglomerates that are then entrained in a jet of compressed air from the gun. The entrained molten material deposits onto the stainless-steel pipe with the compressed air. A rotary motor rotates the pipe in a circular and up-and-down direction to allow for continuous, sequential coating during the 4-hr exposure period within the spray booth (Fig. 3A and B). The spray gun is controlled by computer software and fired at programmed intervals for typically around 25 sprays during the exposure period. During exposure, different physical and chemical properties of the generated aerosols were assessed in the exposure chamber.

3.2. Particle metal composition, morphology, and size

The metal content of the thermal spray coating particles generated using different consumable wires was determined by ICP-AES on bulk samples collected onto filters (Table 2). For the two stainless-steel wires (PMET720 and PMET731), the particles formed were composed of predominantly Fe and Cr. The particles generated when using the PMET731 had nearly double the Cr amount (26.2 %) compared to the particles formed when using the PMET720 wire (13.4 %) at the same spray coating parameters. A change in the compressed air pressure when spray coating with the PMET720 wire appeared to have little effect on metal composition [60 psi: 82.2 % Fe; 13.4 % Cr *vs.* 50 psi: 81.7 % Fe; 14.9 % Cr). Substantially different amounts of Ni were present in the particles when comparing the two Ni-based wire (PMET876 and

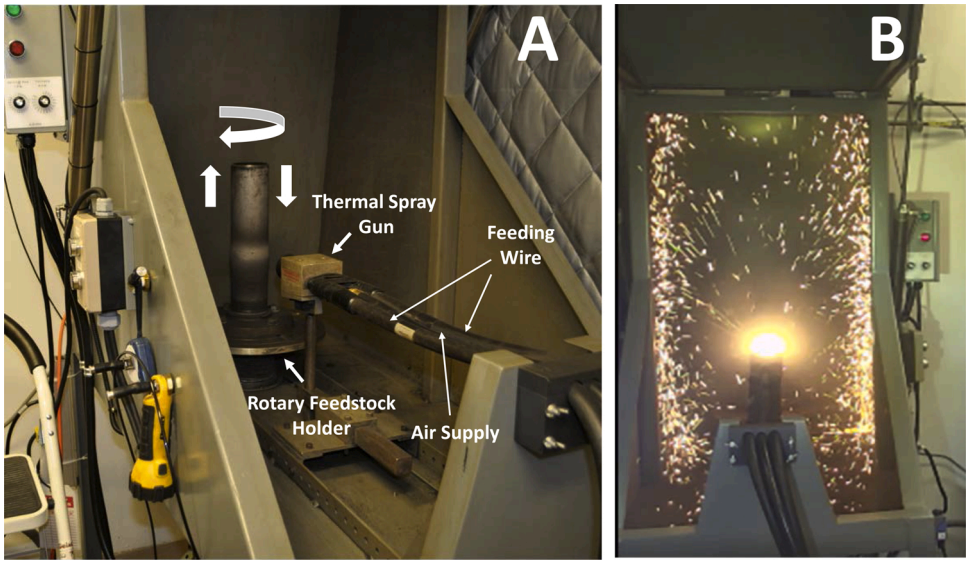

Fig. 3. (A) Image of the stainless-steel pipe to be coated within the spray coating booth (with hood door open) before electric arc- thermal spray coating, showing the thermal spray gun, feeding wire lines, air supply line, rotary holder, and the directions of motion of the pipe. (B) Image of the electric arc-thermal spray coating process. During testing and inhalation exposure studies, the hood door was closed.

PMET885). The particles generated when using PMET885 was composed mostly of Ni (96.9 %) whereas the particles from PMET876 spray coating had less Ni (55.5 %) but significant amounts of Cr (17.4 %), Mo (17.0 %), Fe (5.08 %), and Mn (3.40 %). The particles formed during spray coating using the PMET540 was composed of almost entirely of Zn (99.4 %). SEM-EDX analysis confirmed the ICP-AES results by mapping specific metals of the particle samples generated from all the different wires. Representative SEM micrographs are shown in Fig. 4 and indicated that Zn and Ni were the predominant metals present in the particles using the PMET540 and PMET885, respectively.

The morphology of the generated particles was similar when comparing the different consumable wires (Fig. 5). The particles were arranged as chain-like agglomerates of nanometer-size primary particles. Much larger, micron-size spherical particles also were generated when using each of the wires during spray coating. In the assessment of particle size, representative size distribution graphs for the PMET720 wire using different pressure settings are depicted in Fig. 6 (MOUDI analysis) and 7 (ELPI measurement). The MMAD, geometric standard deviation, and CMAD for PMET720 were comparable when spray coating at either 50 psi or 60 psi (Table 2). The MMAD, geometric standard deviation, and CMAD for all the generated particle samples when using the different wires were similar, ranging from 280 to 378 nm, 1.83–2.13, and 96–165 nm, respectively. Particle surface area as estimated by ELPI software ranged from 3.70×10^5–1.54×10^6 $\mu m^2/cm^3$ (Table 2) (Fig. 7).

3.3. Animal exposure pilot study

In an initial pilot study to test the system, male Sprague-Dawley rats were exposed to the respirable portion of a thermal spray coating aerosol at a target particle concentration of 25 mg/m^3 for 4 h/d for 9 d using a stainless-steel PMET720 wire at 60 psi, 30 V, and 200A. In Fig. 8, a representative computer display of real time measurements within the animal chamber is shown during one 4-hr exposure period, indicating target particle concentration (mg/m^3; dashed orange line), actual particle concentration (mg/m^3; solid red line), CO_2 levels (ppm; solid purple line), each point at which the gun sprays (black dots), and dilution flow rate (L/min; solid green line). Relative humidity (%) and temperature (°F) also were recording during the exposure period. By controlling the number of sprays fired by the gun over time, a mostly consistent target aerosol concentration of 25 mg/m^3 was maintained within the animal exposure chamber during the 4-hr exposure period (Fig. 8; red line). Peaks were observed on the DataRAM recordings immediately after the firing of the spray gun, indicating a rise in aerosol concentration as depicted by the spikes in the red line on the chart. To maintain the target concentration, the spray gun typically fired 25 times during the exposure period as indicted by the black dots on the chart. Each spray lasted for 1 s. The actual measured mean chamber concentration after the 9-d animal exposure was 24.9 mg/m^3 $\pm$ 2.1 standard error. In the example shown in Fig. 8, chamber temperature, relative humidity, and CO_2 levels ranged between 70.6–74.3 ° F, 39.4–67.7 %, and 939.1–4159.3 ppm, respectively. During the 9-d exposure period, established thresholds as set by the institute's animal care and use committee were never exceeded for chamber temperature (79 ° F), relative humidity (70 %), and CO_2 levels (6000 ppm).

At 1 d after the final exposure, BAL was performed on the exposed rats, and markers of lung injury (LDH activity) and inflammation (lung cell differentials) were examined (Fig. 9). In the assessment of lung cell damage, LDH activity in the acellular BALF was significantly higher in the group exposed to thermal spray aerosol as compared to the air control group (Fig. 9A). Also, total cells and AMs recovered by BAL were significantly elevated in the thermal spray coating group compared to air control at 1 d after the final exposure (Fig. 9B&C). No statistical difference was observed between the two groups when comparing the number of PMNs recovered by BAL (Fig. 9D). Also, no significant differences were observed between the two treatment groups when comparing the responses of five common and important cytokines (IL-1α, IL-1β, IL-6, IL-10, and TNF-α) in the BALF involved in the inflammatory response of the lungs (Table 3).

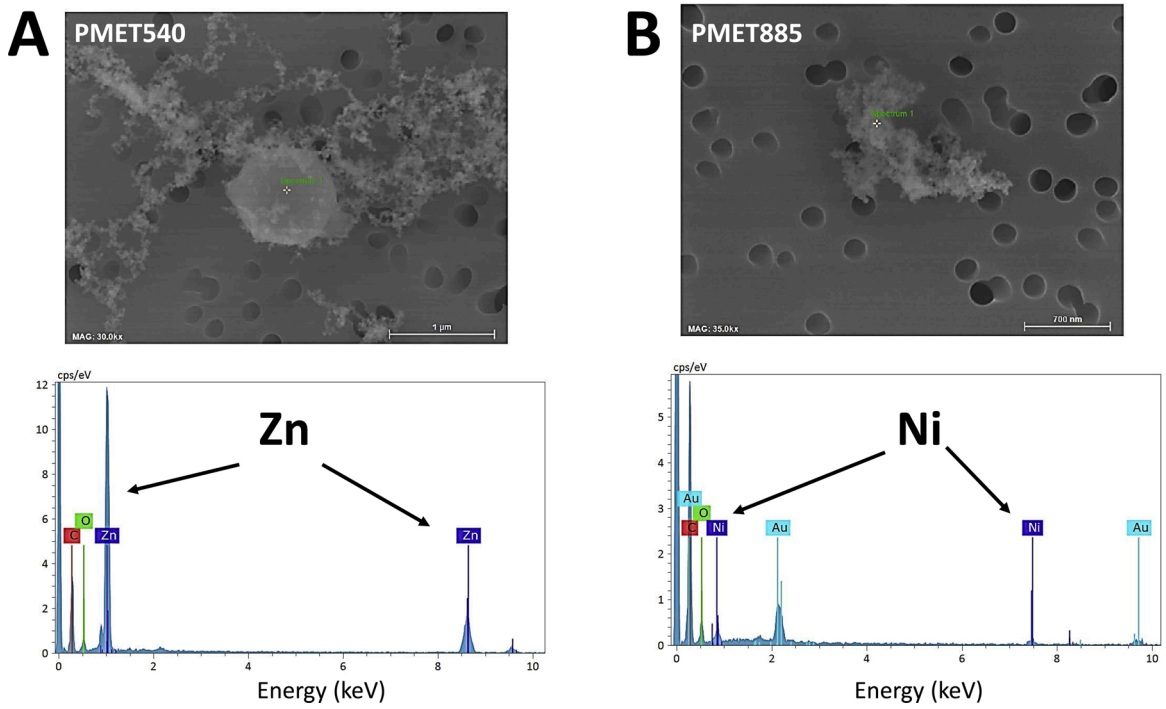

Fig. 4. Representative SEM-EDX image and spectra of particles generated during electric arc thermal spray coating the following consumable wires (A) PMET540, 30,000x magnification and scale bar = 1 µm; (B) PMET885, 35,000x magnification and scale bar = 700 nm. The signal for gold (Au) was derived from the sputter coating process of the collected sample for SEM analysis. Note: the labeled thin vertical lines are guidelines to the positions of the spectral peaks for the elements and should not be confused with the spectra themselves.

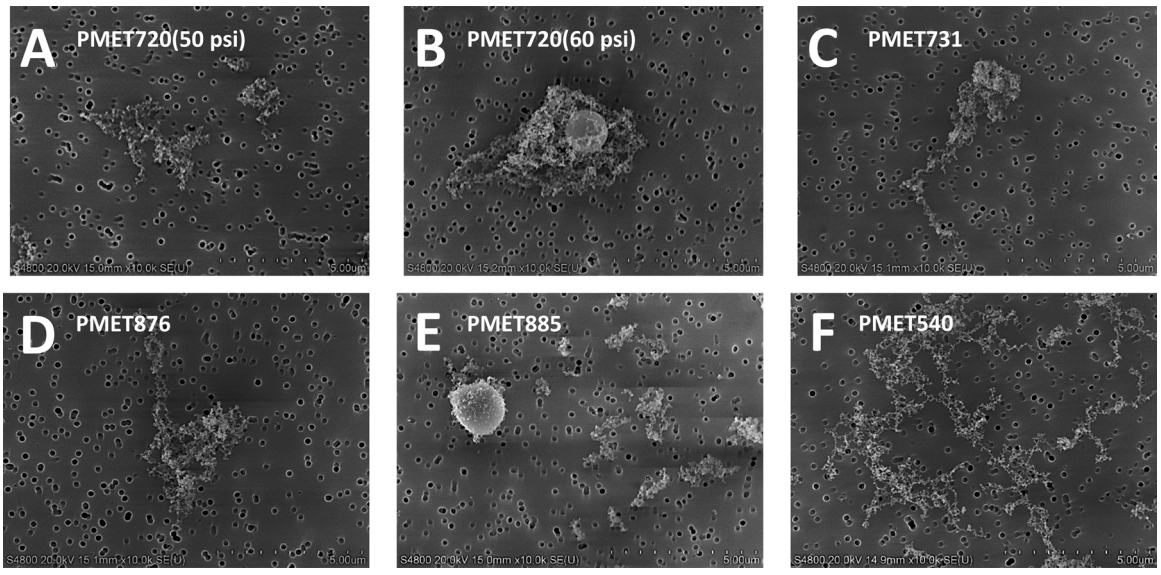

Fig. 5. SEM images of particles generated during electric arc thermal spray coating using the following consumable wires: (A) PMET720 at 50 psi; (B) PMET720 at 60 psi; (C) PMET731; (D) PMET876; (E) PMET885; (F) PMET540. Scale bar = 5 μm.

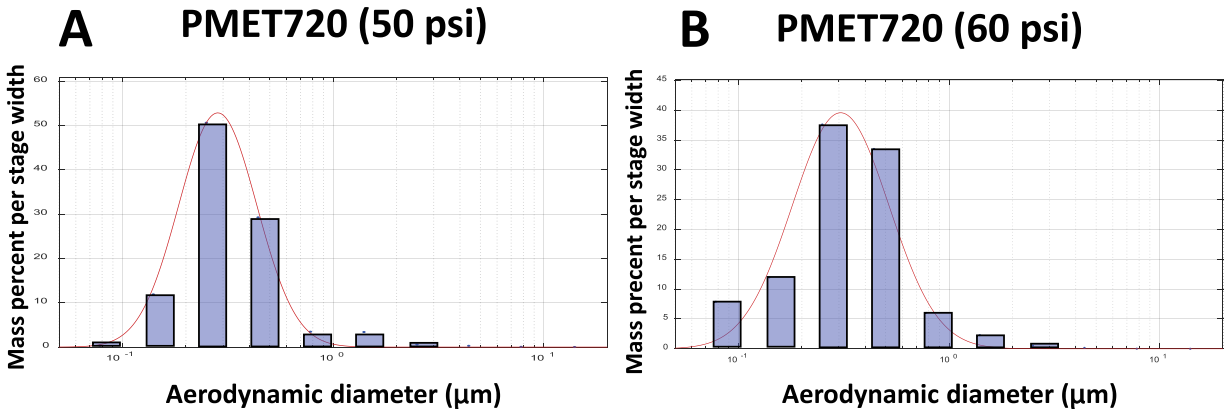

Fig. 6. Representative particle size distribution graphs of generated during electric arc thermal spray coating using the following consumable wires: (A) PMET720 at 50 psi; (B) PMET720 at 60 psi. The mass percent per stage width versus aerodynamic diameter was compared as measured by a Moudi and Nano-Moudi particle sizer. The MMAD for the particles generated using PMET720 at 60 psi was 306 nm with a geometric deviation of 2.11, whereas the MMAD for the PMET 720 at 50 psi was 280 nm with a geometric standard deviation of 1.83.

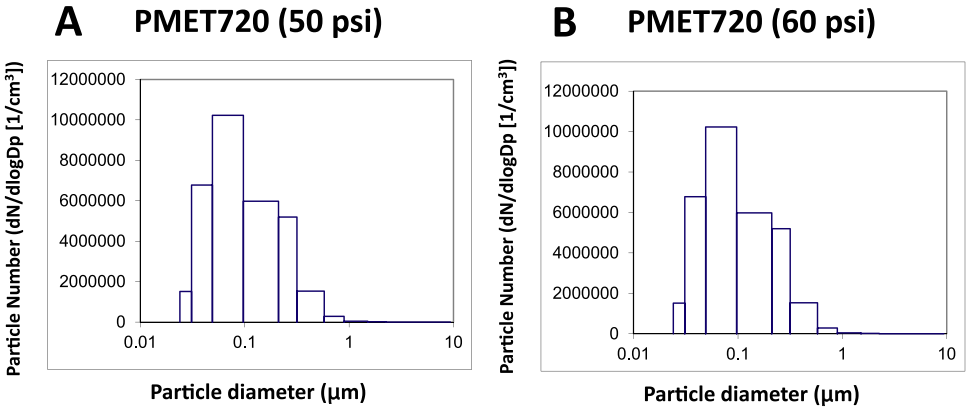

Fig. 7. Representative particle size distribution graphs of generated during electric arc-thermal spray coating using the following consumable wires: (A) PMET720 at 50 psi; (B) PMET720 at 60 psi. The particle number versus particle diameter was compared as measured by an ELPI particle sizer. The CMAD for the particles generated using PMET720 at 60 psi was 103 nm, whereas the MMAD for the PMET 720 at 50 psi was 96 nm.

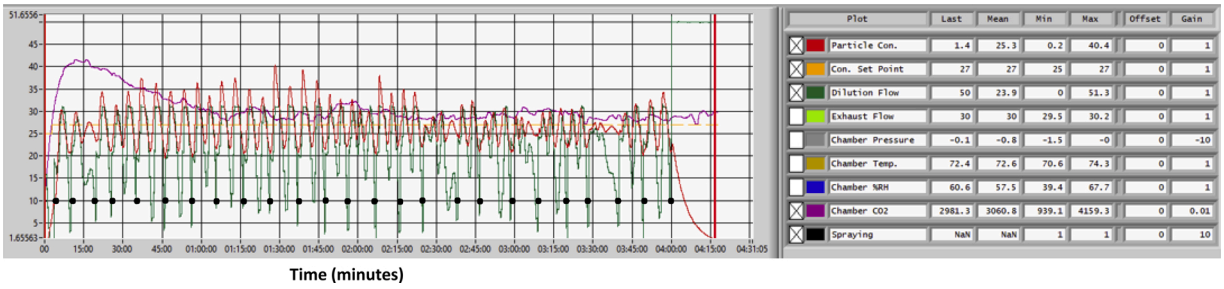

Fig. 8. A representative computer display of real-time measurements of particle chamber concentration (mg/m^3), relative humidity (%), temperature (^{o}F), CO_2 levels (ppm), recording of each spray, and different flow rates (l/min) during a 4-hr spray coating animal exposure using a stainless-steel PMET720 wire at 60 psi, 30 V, and 200A.

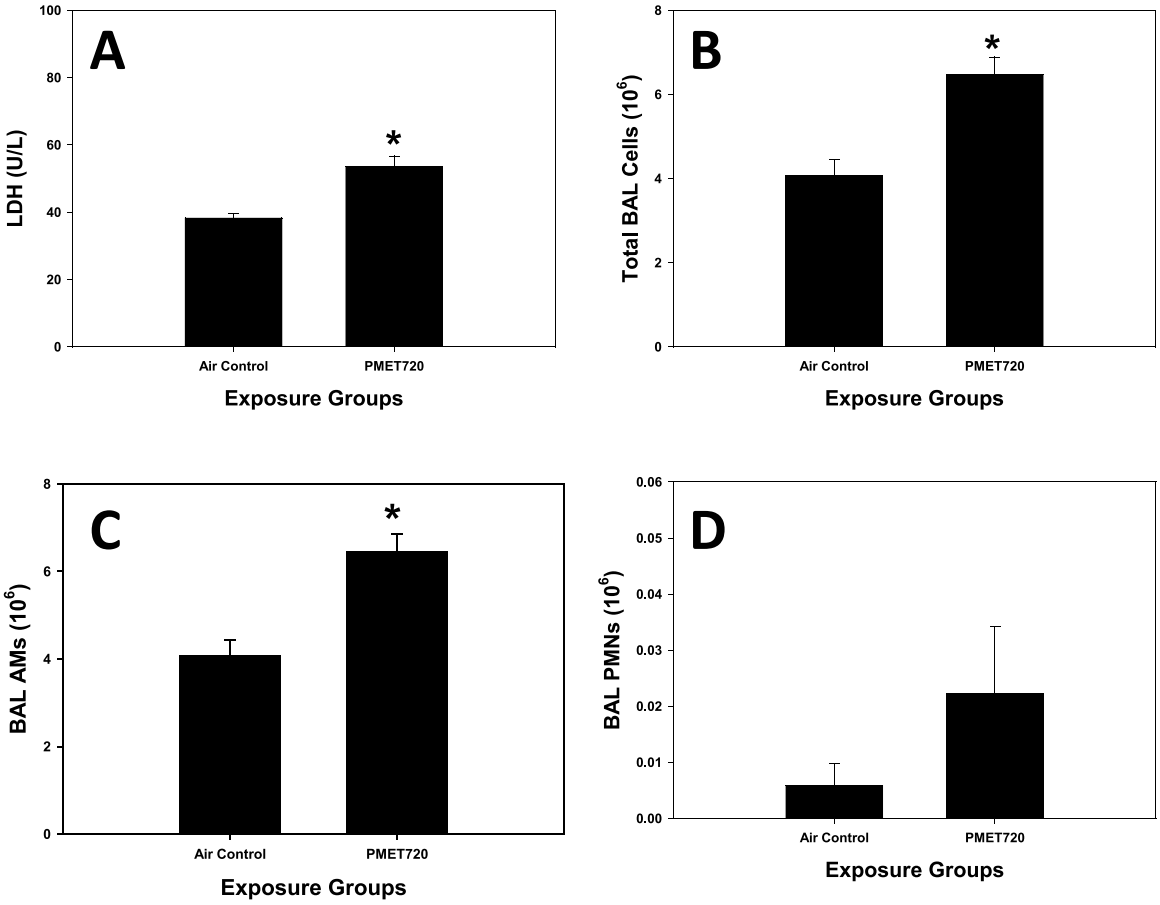

Fig. 9. Lung responses after inhalation to a thermal spray coating aerosol: (A) BAL LDH; (B) Total BAL cells; (C) BAL AMs; (D) BAL PMNs. Male Sprague-Dawley rats (n = 5–6/group) were exposed to the respirable portion of 25 mg/m^3 of electric arc thermal spray aerosol using a PMET720 wire at 60 psi, 30 V, and 200A. The actual measured mean chamber concentration after a 9-d animal exposure (4 h/d) was to be 24.9 mg/m^3 $\pm$ 2.1 standard error; *, Significantly different from air control ($p < 0.05$).

Table 3
Cytokine responses after inhalation to a thermal spray coating aerosol.

Treatment Group	IL-1α (ng/L)	IL-1β (ng/L)	TNF-α (ng/L)	IL-6 (ng/L)	IL-10 (ng/L)
Air Control	0.69 $\pm$ 0.09	0.63 $\pm$ 0.2	0.32 $\pm$ 0.01	15 $\pm$ 0.9	0.68 $\pm$ 0.2
PMET720	0.84 $\pm$ 0.09	0.49 $\pm$ 0.08	0.29 $\pm$ 0.01	18 $\pm$ 2	0.79 $\pm$ 0.2

Note. Male Sprague-Dawley rats (n = 5–6/group) were exposed to the respirable portion of 25 mg/m^3 of electric arc thermal spray aerosol using a PMET720 wire at 60 psi, 30 V, and 200A.

4. Discussion

Elevated levels of potentially toxic and complex metal aerosols are generated during thermal spray coating and have been reported to be as high as 100 times the OSHA permissible exposure limit for the toxic and carcinogenic metal, Cr (A. Siert, Xcel Energy, February, 2017; personal correspondence). High emission rates have been measured for electric arc wire-thermal spray coating that exceed those observed during welding processes. Even inside a well-ventilated workstation, particles concentrations were reported to be higher than 10^8 particles/cm^3 [3]. In agreement, previously reported particle concentrations often exceeded occupational exposure limits particularly, during cleaning and

maintenance of the spray booth and spraying outside or in booths where one-side of a booth was open, ranging from 12.4 mg/m^3–140 mg/m^3 [7,9,23,24].

Like welding fume formation, metal vapors formed during thermal spray coating are transformed into nanometer-size (<100 nm) primary particles that collide and grow into larger, chain-like agglomerates due to the elevated temperatures and turbulent conditions of the process. Both nanometer-size primary particles and micron-size agglomerates have been observed to be formed during different thermal spray coating when using various consumable materials [3,9,13]. It has been reported that up to 90 % of the particles formed during thermal spray coating were smaller than 100 nm [3,13]. In agreement, the particles generated from the different wires during electric arc-spray coating in the current study were arranged as chain-like agglomerates of nanometer size primary particles. Larger, more spherical particles also were formed. This presence of significant amounts of nanoparticles in the generated thermal spray coating aerosols is of importance regarding possible adverse lung responses. Numerous toxicology studies have determined that nanoparticles cause more pulmonary injury and inflammation and have elevated lung deposition when compared based on mass to larger-sized particles of the same composition [14–18]. Also, a difference in the number of nanoparticles in the same stainless-steel welding fume samples generated under varied process parameters were observed to have statistically different lung responses after inhalation exposure in rats [19].

The particle size of these agglomerates, as determined by two different methods (MOUDI and ELPI), did not vary much when using five different consumable wires. MMAD ranged from 280 to 378 nm when measuring size by MOUDI, and the CMAD ranged from 96 to 165 nm when using an ELPI. In the assessment of particle size and emission rates, Viana et al. [20] observed that the properties of the particles generated during thermal spray coating was most likely dependent on the process and not the material. In future studies, it is planned to examine and compare the physical characteristics of aerosols generated during other thermal spray coating processes (e.g., cold spray, plasma spray) to further evaluate whether the process or material has the greatest influence on particle formation.

The metal composition of the generated particles during electric arc wire-thermal spray coating was completely derived from the wire that was consumed during the process. The composition of the stainless-steel pipe that was spray coated did not influence the metal profile of the generated particles. When spray coating using the PMET885 (96.6 % Ni) and PMET540 (99.4 % Zn) wire, the presence of Cr, a significant component of the stainless-steel pipe, was not observed in the formed particles. As determined by ICP-AES, the metal composition of the generated thermal spray coating particles nearly mirrored what was reported to be the composition of the wire by the manufacturer (Table 1), further confirming the source of metal in the resulting profile of the formed particles. For example, PMET885 was measured to be 96.9 % Ni compared to 93.0 %; PMET540 was measured to be 99.4 % Zn compared to 99.9 % Zn; PMET720 was measured to be 82.2 % Fe and 13.4 % Cr compared to 84.7 % Fe and 13.0 % Cr; PMET731 was measured to be 66.3 % Fe and 26.2 % Cr compared to 69.8 % Fe and 23.5 % Cr; and PMET876 was measured to be 55.5 % Ni, 17.4 % Cr, and 17.0 % Mo compared to 60.0 % Ni, 15.0 % Cr, and 16.0 % Mo. In comparison to other metal workplace processes, the composition of welding fume also is derived from the mixture of metals volatilized from the wire/rod or the flux material incorporated within the rod that is consumed during the process [21].

A short-term, animal exposure pilot study was performed to test the system by which male Sprague-Dawley rats were exposed to the respirable portion of 25 mg/m^3 × 4 h/d × 9 d of aerosols generated during thermal spray coating with a PMET720 stainless-steel wire. BALF LDH, a marker of lung injury, and the total number of lung cells recovered by BAL, an index of lung inflammation, were significantly elevated in the group of animals exposed to the thermal spray coating aerosol compared to the control group at 1 d after the last exposure. The increase in total cells in the lungs was due to an influx of AMs, which also was elevated in the thermal spray coating treatment group at 1 d compared to the air controls. There was no significant difference in the number of PMNs recovered from the lungs by BAL when comparing the two groups. Based on these initial findings, it seems likely that stainless-steel thermal spray coating aerosols may pose a risk to the respiratory health of exposed workers.

These observations are not surprising as the lung responses are comparable to the respiratory effects observed in the study of other metal particles that have similar physical and chemical characteristics in terms of size and metal composition to thermal spray coating aerosols. Significant increases in lung injury and inflammation were observed at 1 d after exposure (25 mg/m^3 × 4/h × 8 d) to galvanized and non-galvanized resistance spot welding particles [11,22]. In addition, BALF LDH and recovered AMs, but not PMNs, were significantly increased in rats 1 d after inhalation exposure to gas metal arc- stainless steel (GMA-SS) welding fume at 40 mg/m^3 × 3 h/d × 3 d [10]. However, depending on the parameter measured, the lung responses, including an elevation in PMN influx, did not peak until 6–14 d after exposure to the GMA-SS welding fume. This observation emphasizes the need to examine the temporal lung response at multiple time points after exposure. Studies are currently ongoing that are evaluating the pulmonary effects after inhalation to thermal spray coating aerosols using both stainless-steel and Ni-based wires at time points up to 30 d after different exposure regimens.

To summarize, an automated, thermal spray coating generator and inhalation exposure system was designed and developed. The system is capable of continuously generating a consistent concentration of particles generated during thermal spray coating for an extended period using different consumable wires. The aerosols examined using a variety of different consumable wires were complex metal oxides and arranged as chain-like agglomerates with the primary particles in the nanometer size range. The size distribution of the formed particles as measured by MOUDI and ELPI was multi-modal. A 9-d animal exposure pilot study was completed and indicated that aerosols generated when using a common stainless-steel consumable wire during electric arc-thermal spray coating significantly increased lung injury and inflammation compared to air controls. With the development of this novel thermal spray coating system, dose-response and long-term animal toxicology studies can be easily performed.

Conflict of interest

The authors declare no conflict of interest.

Author statement

All animal experiments complied with National Research Council's Guide for the Care and Use of Laboratory Animals.

Disclaimer

The findings and conclusions in this report are those of the authors and do not necessarily represent the official position of the National Institute for Occupational Safety and Health, Centers for Disease Control and Prevention. Mention of brand name does not constitute product endorsement.

Funding was provided by the National Institute for Occupational Safety and Health project # 93909NE.

Declaration of Competing Interest

The authors report no declarations of interest.

References

[1] ASM Thermal Spray Society, Thermal Spray Technology White Paper Prepared by the Thermal Spray Society Affiliate of ASM International, 2021. Available at http://www.asminternational.org/web/tss/technical/white-paper (Accessed 09/09/2021).

[2] Oerlikon Metco, An Introduction to Thermal Spray- Issue 6, July 2016, Available at https://www.oerlikon.com/ecomaXL/files/metco/oerlikon_BRO-0005.6_Thermal_Spray_Brochure_EN.pdf (Accessed 09/09/2021), 2016.

[3] D. Bemer, R. Regnier, I. Subra, B. Sutter, M.T. Lecler, Y. Morele, Ultrafine particles emitted by flame and electric arc guns for thermal spraying of metals, Ann. Occup. Hyg. 54 (6) (2010) 607–614.

[4] J.M. Antonini, W.G. McKinney, E.G. Lee, A.A. Afshari, Review of the physicochemical properties and associated health effects of aerosols generated during thermal spray coating processes, Toxicol. Ind. Health 37 (2021) 47–58.

[5] Grand View Research, Thermal Spray Coatings Market Size Worth $14.1 Billion by 2028, 2021. Available at https://www.grandviewresearch.com/press-release/global-thermal-spray-coating-market (Accessed 09/09/2021).

[6] U.S. Bureau of Labor Statistics, Occupational Employment and Wages, May 2020: 51-924 Coating, Painting, and Spraying Machine Setters, Operators, and Tenders, Available at https://data.bls.gov/cgi-bin/print.pl/oes/current/oes519121.htm (Accessed 09/09/2021), 2021.

[7] G. Darut, S. Dieu, B. Schnuriger, A. Vignes, M. Morgeneyer, F. Lezzier, F. Derestel, A. Vion, C. Berguery, J. Roquette, O. Le Bihan, State of the art of particle emissions in thermal spraying and other high energy processes based on metal powders, J. Cleaner Prod. 303 (2021), 126952.

[8] NIOSH, Elements by ICP (Hot Block/HCl/HNO_3 digestion): method 7303. NIOSH Manual of Analytical Methods, 4th ed., U.S. Department of Health and Human Services, Washington, DC, 1994. Publication No. 98-119.

[9] H. Huang, H. Li, X. Li, Physicochemical characteristics of dust particles in HVOF spray and occupational hazards: case study in a Chinese Company, J. Thermal Spray Technol. 25 (5) (2016) 971–981.

[10] J.M. Antonini, S. Stone, J.R. Roberts, B. Chen, D. Schwegler-Berry, A.A. Afshari, D. G. Frazer, Effect of short-term stainless steel welding fume inhalation exposure on lung inflammation, injury, and defense responses in rats, Toxicol. Appl. Pharmacol. 223 (2007) 234–245.

[11] J.M. Antonini, A. Afshari, T.G. Meighan, W. McKinney, M. Jackson, D. Schwegler-Berry, D.A. Burns, R.F. LeBouf, B.T. Chen, M. Shoeb, P.C. Zeidler-Erdely, Aerosol characterization and pulmonary responses in rats after short-term inhalation of fumes generated during resistance spot welding of galvanized steel, Toxicol. Rep. 4 (2017) 123–133.

[12] J.M. Antonini, V. Kodali, M. Shoeb, M. Kashon, K. Roach, G. Boyce, T. Meighan, S. Stone, W. McKinney, T. Boots, J.R. Roberts, P.C. Zeidler-Erdely, A. Erdely, Effect of a high fat diet and occupational exposure in different rat strains on lung and systemic responses: examination of the exposome in an animal model, Toxicol. Sci. 174 (2020) 100–111.

[13] A. Salmatonidis, C. Ribalta, V. Sanfelix, S. Benzantakos, G. Biskos, A. Vulpoi, S. Simion, E. Monfort, M. Viana, Workplace exposure to nanoparticles during thermal spraying of ceramic coatings, Ann. Work Expo. Health 63 (1) (2019) 91–106.

[14] D.M. Brown, M.R. Wilson, W. MacNee, V. Stone, K. Donaldson, Size-dependent proinflammatory effects of ultrafine polystyrene particles: a role for surface area and oxidative stress in the enhanced activity of ultrafines, Toxicol. Appl. Pharmacol. 175 (2001) 191–199.

[15] J.S. Brown, K.L. Zeman, W.D. Bennett, Ultrafine particle deposition and clearance in the healthy and obstructed lung, Am. J. Respir. Crit. Care Med. 166 (2002) 1240–1247.

[16] G. Oberdörster, J. Ferin, R. Gelein, S.C. Soderholm, J. Finkelstein, Role of the alveolar macrophage in lung injury—Studies with ultrafine particles, Environ. Health Perspect. 97 (1992) 193–199.

[17] G. Oberdorster, E. Oberdorster, J. Oberdorster, Nanotoxicology: an emerging discipline evolving from studies of ultrafine particles, Environ. Health Perspect. 113 (2005) 823–839.

[18] NIOSH, Progress toward safe nanotechnology in the workplace. A report from the NIOSH Nanotechnology Research Center [DHHS (NIOSH) Publication No. 2007-123], a Progress Report on the Status of Nanotechnology Research Conducted by the NIOSH NTRC through 2006, 2007. Available at http://www.cdc.gov/niosh/docs/2007-123/pdfs/2007-123.pdf (Accessed 01/05/2022).

[19] J.M. Antonini, M. Keane, B.T. Chen, S. Stone, J.R. Roberts, D. Schwegler-Berry, R. N. Andrews, D.G. Frazer, K. Sriram, Alterations in welding process voltage affect the generation of ultrafine particles, fume composition, and pulmonary toxicity, Nanotoxicology 5 (2011) 700–710.

[20] M. Viana, A.S. Fonseca, X. Querol, A. Lopez-Lilao, P. Carpio, Salmatonidis, E. Monfort, Workplace exposure and release of ultrafine particles during atmospheric plasma spraying in the ceramic industry, Sci. Total Environ. 599–600 (2017) 2065–2073.

[21] A.T. Zimmer, P. Biswas, Characterization of the aerosols resulting from arc welding processes, J. Aerosol Sci. 32 (2001) 993–1008.

[22] P.C. Zeidler-Erdely, T.G. Meighan, A. Erdely, J.S. Fedan, J. Thompson, S. Bilgesu, S. Waugh, S. Anderson, N.B. Marshall, A. Afshari, W. McKinney, D.G. Frazer, J. M. Antonini, Effects of acute inhalation of aerosols generated during resistance spot welding with mild steel on pulmonary, vascular, and immune responses in rats, Inhal. Toxicol. 26 (2014) 697–707.

[23] J.K. Chadwick, H.K. Wilson, M.A. White, An investigation of occupational metal exposure in therma spraying processes, Sci. Total Environ. 199 (1997) 115–124.

[24] N. Petsas, G. Kouzilos, M. Vardavoulias, A. Moutsatsou, Worker exposure monitoring of suspended particles ina thermal spray industry, J. Thermal Spray Technol. 16 (2007) 214–219, https://doi.org/10.1007/s11666-007-9027-6.